Int. J. Electrochem. Sci., 7 **(2012)** 2153 - 2163

International Journal of
ELECTROCHEMICAL
SCIENCE
www.electrochemsci.org

Direct Electrochemistry of Glucose Oxidase at Reduced Graphene Oxide/Zinc Oxide Composite Modified Electrode for Glucose Sensor

Selvakumar Palanisamy, A.T. Ezhil Vilian, Shen-Ming Chen[*]

Department of Chemical Engineering and Biotechnology, National Taipei University of Technology, No.1, Section 3, Chung-Hsiao East Road , Taipei 106, Taiwan (R.O.C).
[*]E-mail: smchen78@ms15.hinet.net

Received: 7 January 2012 / *Accepted:* 15 February 2012 / *Published:* 1 March 2012

We prepared the reduced graphene oxide (RGO)/zinc oxide (ZnO) composite on glassy carbon electrode (GCE) by simple and green electrochemical approach. Glucose oxidase (GOx) was immobilized at RGO/ZnO composite modified GCE. The immobilized GOx showed a pair of stable and well-defined reversible redox peaks at the RGO/ZnO composite, with a formal potential ($E^{0'}$) of −0.40 V and a peak to peak separation (ΔE_p) of 70 mV. GOx is strongly adsorbed on the RGO/ZnO composite matrix by the electrostatic interaction between negatively charged GOx and positively charged RGO/ZnO composite. Further, the fabricated glucose biosensor showed good performance over an acceptable linear range from 0.02 to 6.24 mM with a detection limit of 0.02 mM. This composite material could be a promising material for various enzyme based biosensors.

Keywords: Reduced graphene oxide, Zinc oxide, electrocatalysis, Glucose oxidase, Glucose, Biosensors, Electrochemical sensors, Electrochemistry, Bioelectrochemistry

1. INTRODUCTION

Reduced graphene oxide (RGO) is a promising material and recently it has drawn greater attention in various fields. RGO possess unique physicochemical properties like, high surface area [1-3], easy to functionalize with other materials [4] and it owns high conductivity [5]. In recent years, RGO based composites have been used for various applications including biosensor [6], solar cells [7], and super capacitors [8]. On the other hand, glucose oxidase (GOx) based glucose biosensors have been widely used for accurate glucose monitoring. Though GOx has been successfully immobilized on various nanomaterials surface, immobilization of GOx directly on RGO is a challenging task, as they are highly selective [9] and sensitive [10-11]. To date, GOx has been immobilized on the

nanomaterials by various methods, such as physical adsorption [12], and cross-linking [13]. The electrochemical biosensors utilizing metal oxides for glucose biosensing have recently attracted considerable attention. Among various metal oxides, zinc oxide (ZnO) is an exceptional material with high specific surface area, nontoxicity, chemical stability, electrochemical activity, and high electron communication features [14]. At the same time, afore mentioned salient features of RGO and ZnO may provide insight for facile immobilization of GOx aimed for the fabrication of the novel glucose biosensor. Since, ZnO has a high isoelectric point (IEP) of about 9.5, it could be helpful to immobilized GOx (IEP = 4.2) at the RGO/ZnO composite matrix in the physiological pH (7 to 7.4) [15-16]. The positively charged ZnO surface offers a friendly microenvironment for the negatively charged GOx, and the electrostatic interactions between ZnO and GOx helps to retain the bioactivity of GOx. Mean while, the high conductivity of RGO/ZnO promotes the rapid electron shuttling with the FAD redox centre of GOx. Till date, nano and microstructured ZnO has prepared by various methods, such as hydrothermal decomposition [17], thermal evaporation [18] chemical synthesis [19], precipitation method [20], crystallization [21] and electrochemical deposition [22]. Very few reports are available for the fabrication of ZnO nano and microstructures on RGO surface by electrochemical methods that too at elevated temperature (85°C) [22-23].To the best of our knowledge, no reports are available in literature for the room temperature synthesis of ZnO microstructures on RGO surface and for the glucose biosensor applications.

Here, we present a simple, cost-effective, one step electrodeposition of ZnO microflowers on RGO modified glassy carbon electrode (GCE). RGO/ZnO microflowers could be a promising platform to immobilize GOx, as the strong electrostatic interactions between positively charged RGO/ZnO composite and negatively charged GOx could retain its bioactivity. The as-fabricated RGO/ZnO/GOx composite exhibits high electrocatalytic activity towards glucose, which is ascribed to the large surface area as well the synergistic effect of RGO/ZnO composite.

2. EXPERIMENTAL

Graphite powder was purchased from Sigma-Aldrich. GOx, type X-S from Aspergillus niger was purchased from Sigma-Aldrich and used as received. Zinc nitrate hexa hydrate, ($Zn(NO_3)_2.6H_2O$, 99 % pure) and potassium nitrate, (KNO_3) were obtained from Sigma-Aldrich. D(+) glucose (Dextrose, anhydrous) was purchased from Wako pure chemical Industries, Ltd. The supporting electrolyte used for all experiments is pH 5 and 7 phosphate buffer solution (PBS) prepared by using 0.05 M Na_2HPO_4 and NaH_2PO_4 solutions. All the reagents used were of analytical grade and doubly distilled water was utilized for the preparation of all aqueous solutions.

Electrochemical experiments were carried out using a single compartment, three-electrode cell apparatus. All experimental solutions were deoxygenated by passing uncontaminated N_2 gas for 15 min. Cyclic voltammetry (CV) studies were carried out using CHI 750 a work station. GCE (active surface area = 0.079 cm^{-2}) was used as a working electrode and Pt wire with 0.5 mm diameter was used as a counter electrode. All the potentials were referred with respect to standard Ag/AgCl reference electrode. Surface morphological studies were carried out using Hitachi S-3000 H scanning

electron microscope (SEM) and field emission scanning electron microscope (FESEM) by using JSM-6500F field emission scanning electron microscope. Electrochemical impedance spectroscopy (EIS) studies have been performed by using IM6ex ZAHNER (Kroanch, Germany).

2.1 Electrochemical preparation of RGO/ZnO composite

Graphite oxide was prepared by Hummers method [24]. As prepared, purified graphite oxide was dispersed in water, and sonicated for 2 hours to obtain the well exfoliated graphene oxide (GO). As obtained GO (0.5g/ml) was dispersed well in water. Prior to modification, the GCE surface was carefully polished to a mirror finish with alumina slurry and then washed with distilled water and ultrasonicated in water/ethanol for a few minutes. The cleaned GCE was then used for the fabrication of RGO/ZnO/GOx composite film. About 10 µl of GO dispersion was drop casted on the pre-cleaned GCE and dried in air oven at 30°C. Then the GO modified GCE was shifted to an electrochemical cell containing 0.05M $(ZnNO_3)_2.6H_2O$ and KNO_3 solution. 30 successive cyclic voltammograms were performed in the potential range between 0 and -1.5 V at the scan rate of 50 mV s^{-1}. After 30 consecutive cycles, ZnO was electrochemically deposited on RGO modified GCE to form the RGO/ZnO composite.

2.2 Fabrication of RGO/ZnO/GOx composite

Fresh GOx solutions were prepared in PBS and stored at 4 °C when not in use. In order to immobilize GOx on the as-prepared RGO/ZnO composite modified GCE, about 8 µl GOx was drop casted and allowed to dry at room temperature. The negatively charged GOx interacts with the positive charged RGO/ZnO matrix. Thus, immobilization of GOx on RGO/ZnO is highly favored through the electrostatic interactions. The obtained RGO/ZnO composite film modified GCE was then few times gently rinsed with doubly distilled water to remove the loosely bound GOx. The fabricated RGO/ZnO/GOx electrode was used for further experiments. All the electrochemical experiments were carried out at room temperature.

2.3 Mechanism of RGO/ZnO composite formation

In Fig. 1, during the first cycle, a large cathodic peak appears at -1.0 V with a starting potential of -0.75 V. After few cycles, this cathodic peak disappeared completely, due to the reduction of oxygen functionalities at the GO basal plane [25]. Besides that, during the first cycle, with a starting potential of -0.83 V, an anodic peak appears at -0.66 V, indicating that formation of Zinc ions from detachment of the $Zn(NO_3)_2$. Finally, the Zn^{2+} ions reduced to ZnO because of dissociation NO_3^- ions to NO_2^- ions. ZnO electrochemical deposition will occur by the following reversible mechanistic pathways as reported previously, [26-27].

$$Zn^{2+} + NO_3^- + 2e^- \rightarrow ZnO + NO_2^- \quad (1)$$

$$Zn^{2+} + ½\ O_2^{-} + 2e^{-} \rightarrow ZnO \quad (2)$$

In this study, as we maintained the N_2 atmosphere during the entire RGO/ZnO electrochemical deposition process, the ZnO deposition may not have proceeded via step (2). Therefore, ZnO formation should occur via step (1), where Zn^{2+} ions will associate with the oxygen atoms produced by the reduction of NO_3^- ions.

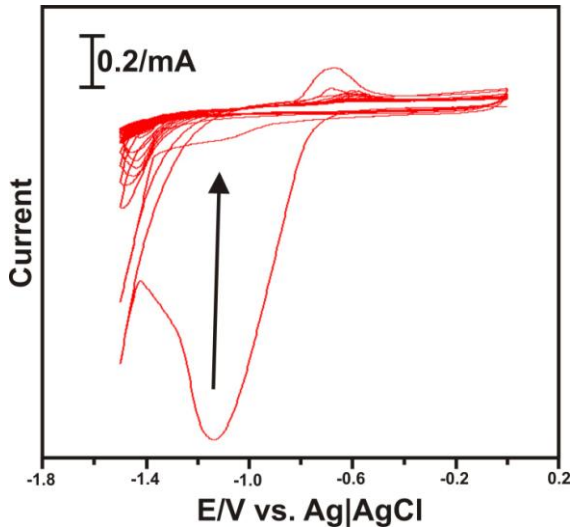

Figure 1. 15 consecutive cyclic voltammograms recorded at a GO-modified GCE in 0.5mM $(ZnNO_3)_2.6\ H_2O$ and 0.5 mM KNO_3 containing N_2 saturated 0.05 M PBS (pH 7) at the scan rate of 50 mV s^{-1}.

During the electrochemical deposition process, the positively charged Zn^{2+} ions from the bath solution will be attracted towards the negatively charged oxygen functionalities of GO via electrostatic attractions, and thus get anchored well at the GO surface. While in the second cathodic potential scan, at more negative potential (~1V), the as dissociated NO_3^- ions will undergo further reduction forming both NO_2^- ions and oxygen. Meanwhile, the released oxygen will be captured immediately by the anchored Zn^{2+} ions, resulting in the formation of RGO/ZnO composite (step 1). Here, it should be noted that, as the Zn^{2+} ions are anchored at GO only via electrostatic force, and as the oxygen present in the functional groups are covalently bonded with the carbon or hydrogen, they may not be involved in the ZnO formation.

3. RESULTS AND DISCUSSIONS

3.1 Direct electrochemistry of GOx

Fig. 2 shows the cyclic voltammograms (CV) obtained at bare, RGO, RGO/ZnO and RGO/ZnO/GOx film modified GCEs in deoxygenated PBS at the scan rate of 50 mV s^{-1}. Cyclic

voltammograms were recorded in the potential range of −0.7 to 0 V. In Fig. 2, RGO/ZnO modified electrode (curve c) has high background current than RGO (curve b).

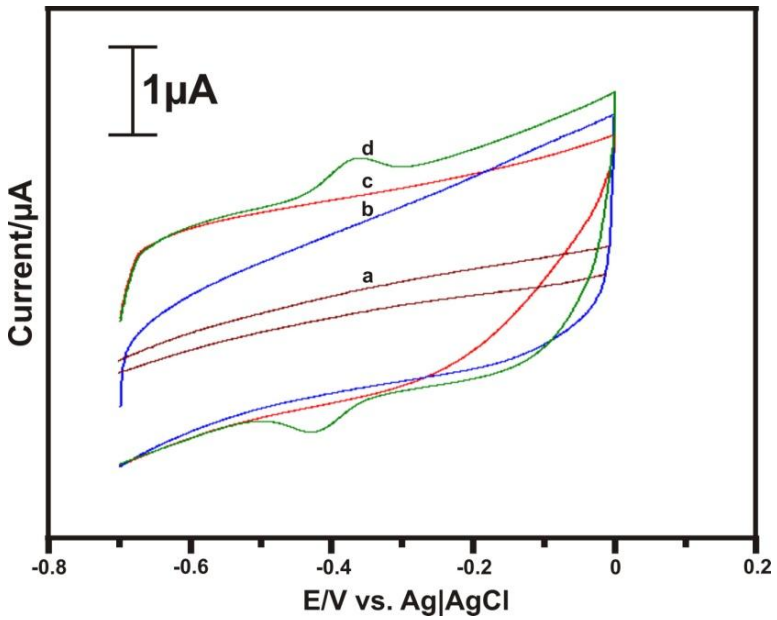

Figure 2. Cyclic voltammograms obtained at bare GCE (a), RGO (b), RGO/ZnO (c), RGO/ZnO/GOx (d) film modified GCEs in deoxygenated PBS at 50 mV s^{-1} scan rate.

It clearly shows that RGO/ZnO has high active electrode area when compared to the RGO modified electrode. In the absence of GOx, no significant redox peaks were noticed in this potential range for bare (curve a,), RGO and RGO/ZnO modified GCEs. However, a pair of well-defined redox peaks was noticed at the RGO/ZnO/GOx modified electrode (curve d,) in the same potential window. The formal potential (E°′) calculated from the average of cathodic and anodic peak potentials was ~-0.43 V (vs standard Ag/AgCl reference electrode). The peak-to-peak separation ratio of cathodic to anodic current intensity was ~70 mV, revealing a fast electron transfer process. It can be concluded that the redox process should be ascribed only to GOx, which is characteristic of reversible electron transfer process of redox active center ($FAD/FADH_2$) in the GOD, and RGO/ZnOs plays a key role in facilitating the direct electron transfer of GOD and the electrode surface. Thus, the direct electron transfer of GOx at RGO/ZnO film has been achieved successfully. The fast electron transfer of GOx can be attributed to the good biocompatibility, large surface area, and high electron communication capability of RGO/ZnO composite.

3.2 Different scan rate studies at RGO/ZnO composite modified electrode

Fig. 3 shows the cyclic voltammograms obtained at RGO/ZnO/GOx composite film modified GCE in deoxygenated PBS at different scan rates. The redox peak currents linearly increased with the scan rates from 10 to 100 mVs^{-1}, the anodic and cathodic peak potentials shifted towards positive and

negative direction, respectively, indicating a surface-controlled quasi-reversible process. The cyclic voltammograms remained essentially unchanged on consecutive potential cycling, which confirmed that GOx is stably immobilized on the RGO/ZnO composite film.

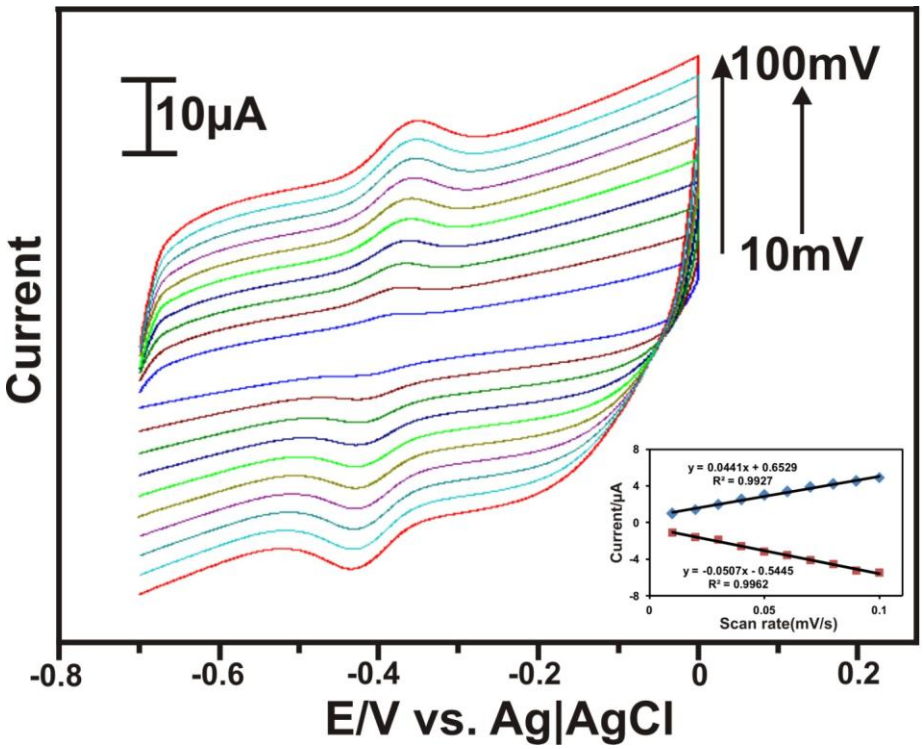

Figure 3. Cyclic voltammograms recorded at RGO/ZnO/GOx composite film modified GCE in deoxygenated PBS at different scan rates. The scan rates from inner to outer are: 10 to 100 mV s^{-1}. Inset shows the linear dependence of I_{pa} (■) and I_{pc} (■) on scan rate (10 to 100 mV s^{-1}).

Fig. 3 inset shows the relationship between cathodic peak potential (I_{pc}) and anodic peak potential (I_{pa}) with scan rate (mV s^{-1}) for RGO/ZnO/GOx. As could be seen, from 10 to 100 mV s^{-1} range, E_{pc} and E_{pa} changed linearly with scan rate, with regression coefficients 0.9927 and 0.9962, respectively

3.3. Effect of pH

It is well known that the direct electrochemistry of GOx, the two-electron and two-proton coupled reaction of the GOx is dependent on the pH solutions. Fig. 4 shows the effect of pH on GOx ($FAD/FADH_2$) redox couple at RGO/ZnO/GOx composite film modified GCE in various buffer solutions (pH 1 to 11). In each pH solution, a pair of stable and well-defined reversible redox peaks of the GOx was observed. Besides, both anodic and cathodic peak potentials are shifted to negative potentials with increasing pH 7-11. Furthermore, in the case of pH to 1-5 solutions, both anodic and cathodic peak potentials shifted towards the positive potential side. In addition, the maximum current response is observed at pH 7. The formal potential of GOx exhibits a linear dependence over wide pH

range (pH 1-11) with a slope of−49.7mV/pH, with the correlation coefficient is 0.9957. This slope value is closer to the theoretical value of Nernstian equation for equal number of proton and electron transfer process [28-29]. This result also validates that, the direct electrochemical reaction of $FAD/FADH_2$ at GOx is a two protons ($2H^+$) and two electrons ($2e^-$) process.

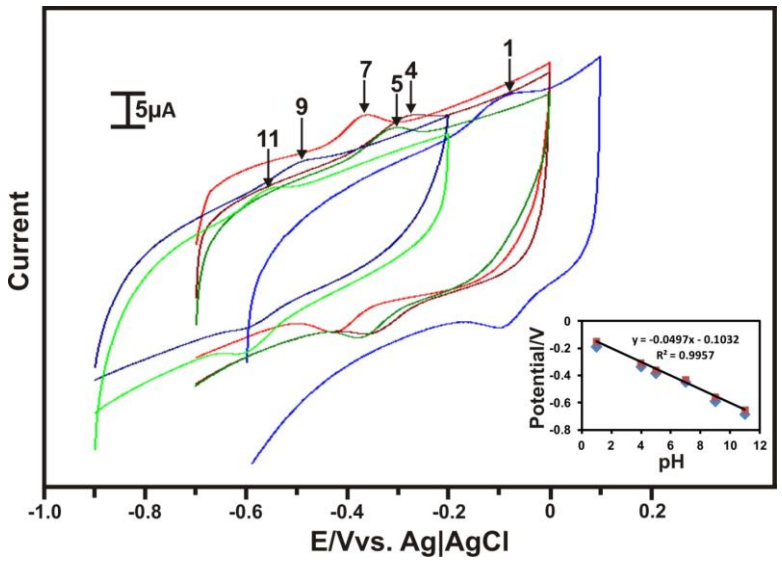

Figure 4. Cyclic voltammograms obtained at RGO/ZnO/GOx composite film modified GCE in deoxygenated various buffer solutions (pH 1–11) at the scan rate of 50 mV s^{-1}. Inset shows the influence of pH on E_{pa} (■), E_{pc} (■) of RGO/ZnO/GOx composite film.

3.4 Electrochemical impedance spectroscopy (EIS) studies

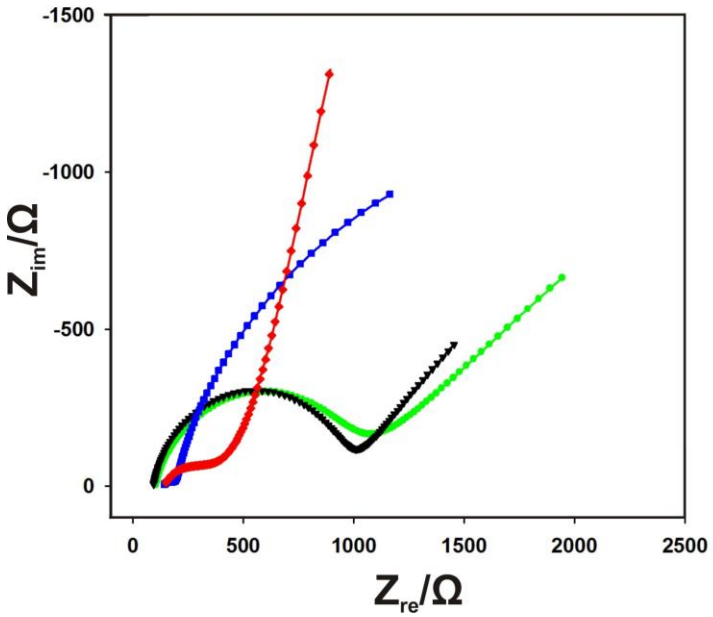

Figure 5. EIS of GOx (●), bare (◥) , RGO/ZnO (◆) and RGO/ZnO/GOx (◆) film modified GCEs in PBS containing 5 mM $Fe(CN)_6^{3-}/Fe(CN)_6^{4-}$. Frequency: 0.1 Hz to 100 kHz.

The EIS measurement is an important tool which provides valuable information about the impedance changes that occur during each electrode modification step [30-32]. The electrochemical impedance behavior at different modified GCE surfaces has been investigated using EIS. Fig. 5 shows the real (Z_{re}) and imaginary part (Z_{im}) of the impedance spectra represented as Nyquist plots for only GOx, RGO/ZnO/GOx, RGO, and RGO/ZnO modified GCEs in PBS containing 5 mM $Fe(CN)_6^{3-/4-}$. GOx modified GCE (●) possess higher electron transfer resistance (R_{et}) value than bare GCE (◥). The reason for the poor electron transfer at the former can be due to the reason that FAD redox centre is not easily accessible as it is deeply located inside the GOx. Fascinatingly, a depressed semicircle is observed at RGO/ZnO/GOx GCE electrode (◆), indicating the fast electron transfer process. This can be ascribed to the excellent conductivity of RGO/ZnO (◆) composite which is evident from the small semicircle and its corresponding lower R_{et} value. EIS results show that, RGO/ZnO/GOx modified electrode exhibits rapid electron transfer than the GOx and unmodified GCEs, because of the existence of highly conductive RGO and ZnO.

3.5. Surface morphology of RGO/ZnO/GOx modified electrode

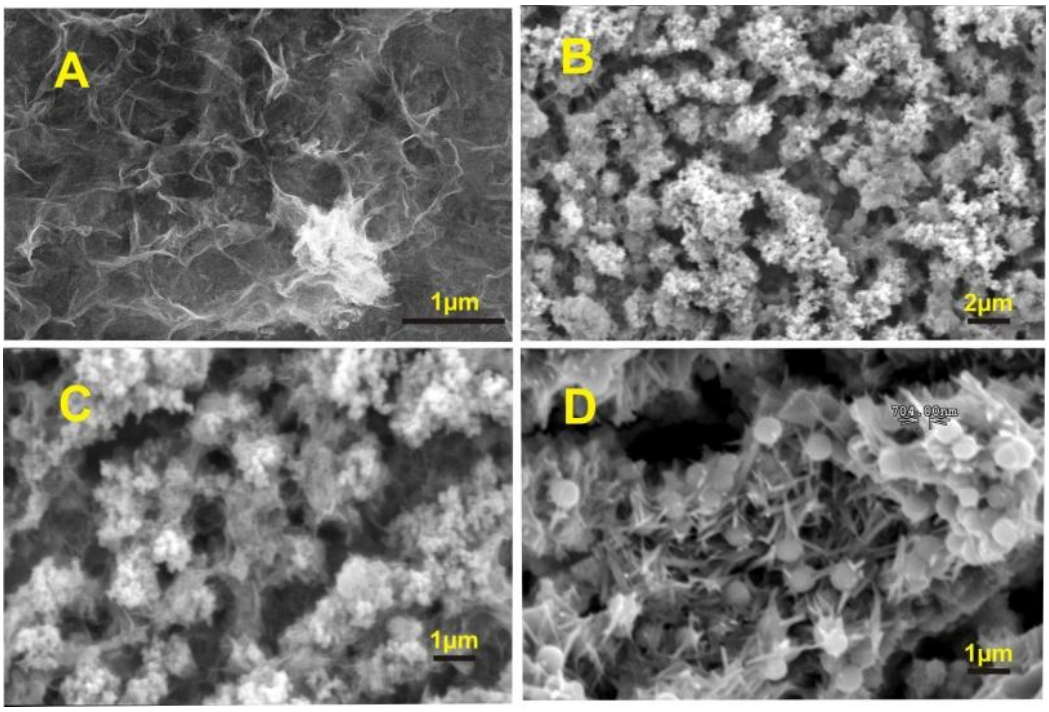

Figure 6. FESEM image of RGO (A), SEM images of electrochemically prepared RGO/ZnO composite at different magnifications (B and C). RGO/ZnO/GOx film (D)

Fig. 6A shows a typical FESEM image of the as-electrochemically prepared RGO. It can be seen that the nanosheets are wrinkled and they are uniform in size. Fig. 6B and 6C shows the electrochemically deposited zinc oxide micro-flowers on the RGO surface at different magnifications. Here, we can be seen that ZnO micro-flowers are uniform in size (500 nm-1 µm). RGO sheets possess branched networks which connect and anchor the zinc oxide micro flowers closely. It is notable that

both ZnO and RGO morphology has been retained in the composite film and they are successively fabricated electrochemically. Fig. 6D shows that GOx microspheres are anchored firmly on the composite matrix through the electrostatic interactions. SEM results validate that, RGO/ZnO composite material is a promising platform for the GOx immobilization.

3.6 Electrocatalysis of oxygen and glucose at the RGO/ZnO/GOD modified electrode

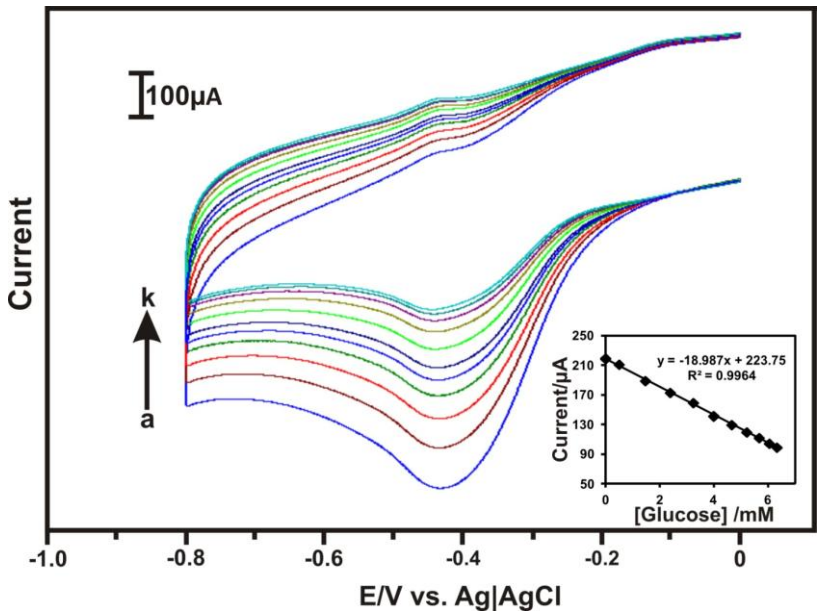

Figure 7. Cyclic voltammograms recorded at RGO/ZnO/GOx composite film modified GCE (a) without and (b-k) with 0.02 - 6.24 mM glucose containing oxygenated PBS. Scan rate: 50 mV s^{-1}. Inset plot shows the linear dependence of peak current vs. [glucose]/mM for RGO/ZnO/GOx (■) film modified GCE.

RGO/ZnO composite exhibited good electrocatalysis toward the reduction of O_2 and oxidation of glucose. Figure 7 shows the cyclic voltammograms obtained at RGO/ZnO/GOx modified electrode in 0.05 M PBS solution with different concentrations of glucose (saturated with O_2). The reduction current decreased linearly with the addition of glucose in the solution, because of the reduction of oxygen from the solution [33-34]. Moreover, the calibration curve corresponding to cyclic voltammetry response (as inset in Figure 7) is linear against the concentrations of glucose ranging from 0.02 to 6.24 mM with correlation coefficients of 0.996. This result shows that the composite film possesses higher electrocatalytic activity for glucose. The catalytic reduction current observed at the composite film[35-37] significantly decreases with increasing the glucose concentration (a-k), indicating excellent catalytic activity for glucose. The sensitivity obtained from the calibration plot is 18.97 μAmM^{-1}. The composite film has good electrocatalytic response in the linear concentration range from 0.02 to 6.24 mM of glucose.

The stability of RGO/ZnO composite GOx film was studied by recording consecutive cyclic voltammograms at the modified GCE in N_2 saturated 0.05 M PBS (pH 7). The background current was

92% stable even after 400 consecutive cycles, which indicates the excellent stability of the GOx at the composite film. The good stability of the RGO/ZnO/GOx composite film can be attributed to the strong electrostatic interactions between GOx and the composite matrix.

4. CONCLUSIONS

In summary, we present the simple and cost effective one step electrodeposition of ZnO microflowers on RGO modified glassy carbon electrode (GCE). The SEM images of RGO/ZnO composite films revealed that ZnO micro flowers are well formed, and anchored well at the surface of graphene sheets. RGO/ZnO microflowers are a wonderful platform to immobilize GOx for glucose biosensor. The strong electrostatic interactions between positively charged RGO/ZnO composite and negatively charged GOx provides good stability to the immobilized GOx. The as-prepared RGO/ZnO/GOx composite film showed good catalytic activity for glucose oxidation. Besides that, RGO/ZnO sensor is highly sensitive towards glucose and it holds acceptable stability. As a future perspective, we believe that RGO/ZnO composite material could be a promising electrode material for the fabrication of various enzyme based biosensors, super capacitors and solar cells at low cost.

ACKNOWLEDGEMENT
This work was supported by the National Science Council and the Ministry of Education of Taiwan (Republic of China). I am very much thankful to Dr. Arun Prakash Periasamy for his timely help and valuable suggestions.

References

1. L. Zhang, Y. Li, L. Zhang, D.W. Li, D. Karpuzov, Y.T. Long, *Int. J. Electrochem. Sci*., 6 (2011) 819 – 829.
2. A.Galal, N F. Atta, H. K. Hassan, *Int. J. Electrochem. Sci*., 7 (2012) 768 – 784.
3. S. Stankovich, D.A. Dikin, R.D. Piner, K.A. Kohlhaas, A. Kleinhammes, Y. Jia, Y. Wu, S.B.T. Nguyen, R.S. Ruo, *Carbon* 45 (2007) 1558–1565.
4. Y. Shao, J. Wang, H. Wu, J. Liu, I.A. Aksay, Y. Lin, *Electroanalysis* 22 (2010) 1027 – 1036.
5. M.D. Stoller, S. Park, Y. Zhu, J. An, R.S. Ruoff, *Nano Lett*., 8 (2008) 10.
6. Z. Wang, X. Zhou, J. Zhang, F. Boey, H. Zhang, *J. Phys. Chem*. C, 113 (2009) 14071–14075.
7. V.K. Rana, M.C. Choi, J.Y. Kong, G. Y Kim, M.J. Kim, S.H Kim, S. Mishra, R.P Singh, C.S. Ha, *Macromol. Mater. Eng*. 296 (2011) 131–140.
8. X. Wang, L. Zhi, K. Mullen, *Nano Lett*. 8 (2008) 323-327.
9. D. Lee, J. Lee, J. Kim, H.B. Na, B. Kim, C.H. Shin, J.H. Kwak, A. Dohnalkova, J.W.Grate, T. Hyeon, H.S. Kim, *Adv.Mater*. 17 (2005) 2828–2833.
10. X.L. Luo, J.J. Xu, Y. Du, H.Y. Chen, *Anal. Biochem*. 334 (2004) 284–289.
11. W. Zhao, J.J. Xu, C.G. Shi, H.Y. Chen, *Langmuir* 21 (2005) 9630–9634.
12. F. Battaglini, P. N. Bartlett, J. H. Wang, *Anal. Chem*. 72 (2000) 502.
13. J. J. Burmeister, G. A. Gerhardt, *Anal. Chem*. 73 (2001) 1037.
14. X. W. Sun, H. S. Kwok, *J. Appl. Phys*. 86 (1999) 408.

15. F. F. Zhang, X. L. Wang, S. Y. Ai, Z. D. Sun, Q. Wan, Z. Q. Zhu, Y. Z. Xian, L. T. Jin, K. Yamamoto, *Anal. Chim. Acta*. 519 (2004) 155.
16. J. Zang, C.M. Li, X. Cui, J. Wang, X. Sun, H. Dong, C.Q. Sun, *Electroanalysis* 19 (2007) 1008 – 1014.
17. B. Fang, C. Zhang, G. Wang, M. Wang, Y. Ji, *Sens. Actuators*, B, 155 (2011) 304–310.
18. A. Wei, X.W. Suna, J. X. Wang, Y. Lei, X.P. Cai, C.M. Li, Z.L. Dong, W. Huang, *Appl. Phys. Lett*. 89 (2006) 123902.
19. X. Ren, D. Chen, X. Meng, F. Tang, X. Hou, D. Han, L. Zhang, *J. Colloid Interface Sci*. 334 (2009) 183– 187.
20. J. Wang, Z. Gao, Z. Li, B. Wang, Y. Yan, Q. Liu, T. Mann, M. Zhang, Z. Jiang, *J. Solid State Chem*. 184 (2011) 1421–1427.
21. L. Zhang, Z. Chen, Y. Tang, Z. Jia, *Thin Solid Films* 492 (2005) 24 – 29.
22. T. Kong, Y. Chen, Y. Ye, K. Zhang, Z. Wang, X. Wang, *Sens. Actuators*, B, 138 (2009) 344–350.
23. Y.L. Chen, Z.A. Hu, Y.Q. Chang, H.W. Wang, Z.Y. Zhang, Y.Y. Yang, H.Y. Wu, *J. Phys. Chem*. C 115 (2011) 2563–2571.
24. W.S. Hummers, R.E. Offeman, *J. Am. Chem. Soc*., 80 (1958) 1339.
25. H.L. Guo, X.F. Wang, Q.Y. Qian, F.B. Wang, X.H. Xia, *Nano Lett*. 3 (2009) 2653–2659.
26. M. Izaki, T. Omi, *Appl. Phys. Lett*. 68 (1996) 17.
27. M. Izaki, T. Omi, *J. Electrochem. Soc*. 143 (1996) 25.
28. N. Jia, L. Liu, Q. Zhou, L. Wang, M. Yan, Z. Jiang, *Electrochim. Acta* 51 (2005) 611–618.
29. D. Wen, Y. Liu, G. Yang, S. Dong, Electrochim. Acta 52 (2007) 5312–5317.
30. C. Shan, H. Yang, J. Song, D. Han, A. Ivaska, L. Niu, *Anal. Chem*. 81 (2009) 2378–2382.
31. S.W. Ting, A.P. Periasamy, S.M. Chen, R. Saraswathi, *Int. J. Electrochem. Sci*., 6 (2011) 4438 - 4453
32. S.Yu Liu, J. Xie, Q. Pan, C.Y. Wu, G.S. Cao, T.J. Zhu, X.B. Zhao, *Int. J. Electrochem. Sci*., 7 (2012) 354 - 362
33. R. Garjonyte, A. Malinauskas, *Sens. Actuators* B, 56 (1999) 85–92.
34. A.P. Periasamy, Y.J. Chang, S.M. Chen, *Bioelectrochemistry*, 80 (2011) 114–120.
35. K.C. Lin, S.M. Chen, *Biosensors and Bioelectronics*, 21 (2006) 1737-1745
36. S. A. Kumar, H.W. Cheng, S.M. Chen, *Reactive and Functional Polymers*, 69 (2009) 364-370.
37. K.C. Lin, S.M. Chen, *J. Electroanal. Chem.*, 578(2005) 213-222.